Annals of Biomedical Engineering, Vol. 38, No. 1, January 2010 *(© 2009)* pp. 66–76
DOI: 10.1007/s10439-009-9834-7

The Glenohumeral Capsule Should be Evaluated as a Sheet of Fibrous Tissue: A Validated Finite Element Model

SUSAN M. MOORE,[1] BENJAMIN ELLIS,[2] JEFFREY A. WEISS,[2] PATRICK J. MCMAHON,[1] and RICHARD E. DEBSKI[1]

[1]Musculoskeletal Research Center, Department of Bioengineering, University of Pittsburgh, 405 Center for Bioengineering, 300 Technology Drive, Pittsburgh, PA 15219, USA; and [2]Department of Bioengineering, University of Utah, Salt Lake City, UT, USA

(Received 1 October 2008; accepted 28 October 2009; published online 13 November 2009)

Abstract—The function of the glenohumeral capsule has typically been evaluated by isolating several discrete, ligamentous regions during experimental and computational investigations. However, recent data suggests that the regions of the glenohumeral capsule have significant interactions and function multiaxially. Therefore, examining the function of the inferior glenohumeral ligament as a discrete structure may not be appropriate. The objective of this work was to validate the predicted strain distribution and deformed shape of the inferior glenohumeral ligament using experimental data for two subject-specific finite element models: (1) a continuous model including all capsular regions, and (2) a discrete model including only the inferior glenohumeral ligament. The distribution of maximum principal strain and deformed shape of the glenohumeral capsule was determined for a cadaveric shoulder in a joint position frequently associated with dislocation (60° of glenohumeral abduction, 52° of external rotation, and a 25 N anterior load applied to the humerus). The experimental kinematics were then applied to the two finite element models constructed from the geometry and material properties from the same cadaveric shoulder and the predicted strain distributions and deformed shapes were determined. For the continuous model, the average difference between predicted strains and experimental strains was less than 5%. The predicted deformed shape was also similar to experimental data, with the anterior band of the inferior glenohumeral ligament clearly wrapped around the humeral head. In contrast, large differences existed between the strains predicted by the discrete model when compared to the experimental strains for this joint position (average difference from experimental data was 20%). In addition, the predicted deformed shape of the inferior glenohumeral ligament did not wrap around the humeral head. These differences may be attributed to neglecting the complex interactions between the anterior band of the inferior glenohumeral ligament with the neighboring capsular regions. Thus, the glenohumeral capsule should not be evaluated as several discrete structures. Rather, it should be evaluated as a single sheet of fibrous tissue.

Keywords—Shoulder, Strain, Kinematics.

Address correspondence to Richard E. Debski, Musculoskeletal Research Center, Department of Bioengineering, University of Pittsburgh, 405 Center for Bioengineering, 300 Technology Drive, Pittsburgh, PA 15219, USA. Electronic mail: genesis1@pitt.edu

INTRODUCTION

Greater than 80% of glenohumeral joint dislocations occur in the anterior direction,[10,21] resulting in injury to the inferior glenohumeral ligament.[2,3,9,17,25,35] Clinical exams for diagnosis of injury and surgical planning apply an anterior load to the humerus and assess the magnitude of anterior translation. Excessive translation indicates that an injury to the inferior glenohumeral ligament of the capsule, which is a passive stabilizer for motions in the anterior direction, has occurred. These clinical exams are performed with the joint oriented in approximately 60° of glenohumeral abduction, with the humerus in the scapular plane, and at various degrees of external rotation (e.g. 60° of external rotation). Surgical planning to repair tissue injured during dislocation includes making a general assessment as to the quantity of capsular tissue that will likely need to be shifted or plicated to restore joint stability.[15,40,43] Typically, the tissue involved in the procedure is largely composed of the inferior glenohumeral ligament.

While surgical repair is often advocated, nearly a quarter of patients experience redislocations following these surgical repair procedures.[41] These poor clinical outcomes may be attributed to a limited understanding of the biomechanical function of the capsular regions. Due to the complex nature of the glenohumeral capsule (Fig. 1), research has primarily focused on evaluating the tensile properties and function of the capsular regions in the direction parallel to their longitudinal axis after isolating them into discrete entities.[4–6,13,16,24,32,33,36,42] However, a number of recent studies have indicated that the functional role of the glenohumeral capsule is complex and muli-axial.[12,14,29,30,32,33] Therefore, it may be inappropriate to evaluate the mechanical properties and function of the capsular regions only in the direction parallel to their longitudinal axis.

In our research center, we have begun to develop methodologies to construct and validate subject-specific

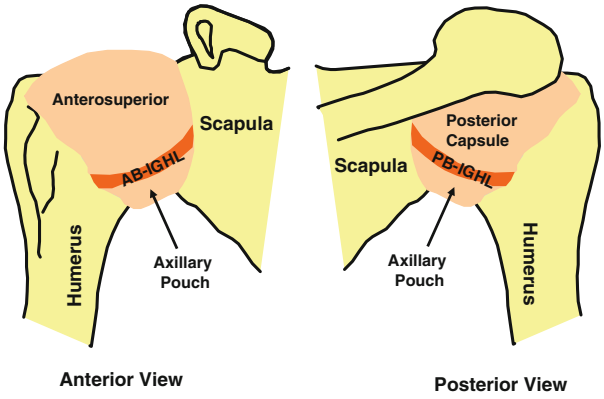

FIGURE 1. Schematic denoting capsular regions of the glenohumeral joint of a right shoulder.

finite element models of the glenohumeral capsule.[13,16] Using the finite element method, the function of each capsular region may be evaluated multi-axially at various joint positions or under various loading conditions by analyzing the resulting strain distributions. The stress distributions in the glenohumeral capsule, reaction forces at the attachment sites of the glenohumeral capsule to the humerus and scapula, and contact forces generated as the glenohumeral capsule wraps around the articular surface of the humeral head may also be determined. Our previous work has established the experimental methodologies necessary to validate the strain predictions from finite element models of the glenohumeral joint.[32] However, previous computational studies have modeled the regions of the capsule as discrete structures[13,16] and have not attempted to construct and validate a computational model of the glenohumeral capsule whereby all the capsular regions are included simultaneously. In other words, a finite element model that represents the capsule as a continuous sheet of tissue with all capsular regions rather than just a finite element model of only one discrete capsular region has not been constructed and validated.

The effect of evaluating each capsular region independent of the remaining capsular regions is unknown. One explanation for this lack of knowledge is the difficulty associated with constructing and validating experimental or computational models that include all capsular regions as opposed to only the region of interest. For example, several experimental inputs are needed for finite element models such as the mechanical properties and geometry for all capsular regions. Furthermore, since the capsular regions function multi-axially, excluding neighboring capsular regions would likely affect the complex interactions between the capsular regions of interest and suggests that the function of the inferior glenohumeral ligament cannot be properly examined when it is modeled as a discrete structure. Therefore, the objective of this study was to validate the predicted strain distribution and deformed shape of the inferior glenohumeral ligament for two subject-specific finite element models: (1) continuous model that included all capsular regions as one sheet of tissue and (2) discrete model that included only the inferior glenohumeral ligament. Experimental strain data was utilized for validation purposes. The findings of this study could have implications for experimental and computational models that examine the function of the glenohumeral capsule. Validated computational models could be utilized to evaluate the effect of diminished mechanical properties on the stress, strain, and force transmission of the capsular regions.

METHODS

Overview of Methodology

Two subject-specific finite element models were constructed based on one cadaveric shoulder. The experimental inputs to the models included: (1) geometry of capsular regions, humerus, and scapula; (2) mechanical properties of capsular regions; and (3) joint kinematics during a simulated clinical exam. Additionally, the strain distribution in the inferior glenohumeral ligament was experimentally measured during the joint kinematics. For validation, the predicted strain distributions and deformed shape were compared to these experimental data.

Specimen Preparation

One fresh-frozen cadaveric shoulder specimen (male, 45 years old, left) was stored at −20 °C and allowed to thaw at room temperature overnight. All soft tissues were dissected away except for the glenohumeral capsule and the coracohumeral ligament. Radiographs and dissection verified that signs of osteoarthritis or previous injury were not present. Special care was taken to ensure that the glenohumeral capsule remained hydrated with a 0.9% physiologic saline solution during the dissection and experiments.

Black plastic strain markers were then fixed to the inferior glenohumeral ligament to determine a reference strain configuration for the entire glenohumeral capsule based on the method reported by Malicky and coworkers.[30] The margins and insertion sites of the anterior and posterior bands of the inferior glenohumeral ligament were identified and a 7 × 11 grid of strain markers (1.58 mm diameter, ~5 mm between strain markers) was adhered to the capsule using cyanoacrylate (Fig. 2). The first column of markers was

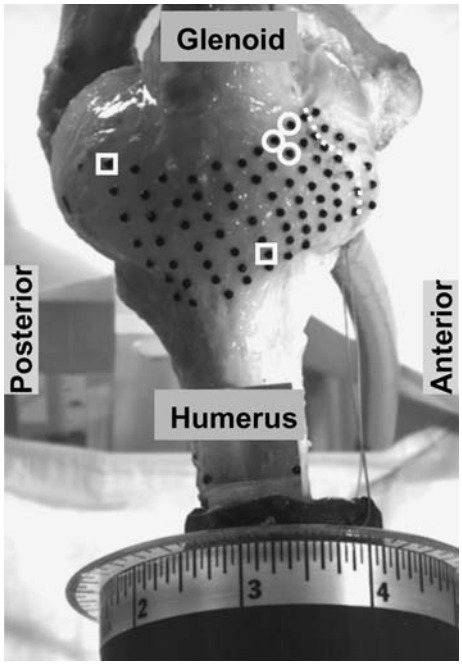

FIGURE 2. Inferior view of the left shoulder showing the glenohumeral capsule in the reference strain configuration with the joint at 10° of external rotation (white dotted line indicates AB-IGHL; white circle indicates strain markers that became detached from the capsule during the experimental protocol; white squares indicate strain markers that remained on the capsule during experimental protocol but were not rigidly attached).

placed just superior to the anterior band of the inferior glenohumeral ligament and the first and last strain markers in each column were approximately 1 cm from the bony insertion sites. Due to the size of the axillary pouch, the 11th column of strain markers was just below the inferior margin of the posterior band of the inferior glenohumeral ligament. A 2 × 4 grid of strain markers was then affixed to the anterosuperior and posterior capsular regions. Plexiglas blocks (Midwest Game Supply Company, 20 × 20 mm) were also affixed to the humerus and scapula using a cyanoacrylate and baking soda compound to allow definition of local coordinate systems for co-registration of specimen geometry and kinematic data. The humerus was potted in a cylinder of epoxy putty, and the scapula was fixed in a block of epoxy putty for mounting in a robotic/universal force-moment sensor testing system.

Experimental Data

A reference strain configuration for all of the capsular regions was subsequently determined.[30,34] This methodology removes the folds and wrinkles in the glenohumeral capsule while it is inflated with compressed air. The joint was mounted within a 6-degree of freedom plastic jig at 60° of glenohumeral abduction and neutral (in the plane of the scapula) horizontal abduction and internal/external rotation. A small amount of joint distraction was then applied to remove some of the folds in the glenohumeral capsule. The glenohumeral capsule was subsequently inflated with compressed air via a needle placed through the rotator interval. A preliminary study indicated that obtaining the reference strain configuration for the anterosuperior region, posterior region, and inferior glenohumeral ligament required that the glenohumeral capsule be inflated to a minimum pressure of 4.8 kPa and a maximum pressure of 6.2 kPa. Thus, the glenohumeral capsule was inflated to the maximum and minimum pressures as the humerus was moved to 0°, ±5°, ±10°, and ±15° of internal/external rotation in a random order. At each joint position, the location of the strain markers were recorded for both pressures using a 3-camera custom built motion tracking system (Spicatec, HI; accuracy: ±0.08 mm, repeatability: ± 0.07 mm) which had been calibrated for a camera configuration that ensured each strain marker would be visible by at least two cameras at all times. The joint orientation corresponding to the smallest average motion of the strain markers between each pressure with no marker moving more than 1 mm, was then selected. The joint orientation selected was 10° of external rotation with a maximum strain marker motion of 0.30 mm. At this joint orientation, the reference strain configuration was determined by inflating the glenohumeral capsule to 5.2 kPa, which removed all folds and wrinkles, and recording the location of the strain markers.

After the reference configuration was determined, a clinical exam was simulated and the locations of the strain markers in the strained configuration were recorded. Using the locations of the markers in the reference and strained configurations, the maximum principal strains in the mid-substance of the inferior glenohumeral ligament were calculated.[34] To simulate the clinical exam, the shoulder was mounted in a robotic/universal force-moment sensor testing system.[7,8,14] The humerus was secured within a thick-walled aluminum cylinder and fixed in a custom clamp mounted to the base of the system. The scapula was rigidly attached to the end-effector of the manipulator through another specially designed clamp and the universal force-moment sensor. The coordinate system of the robotic/universal force-moment sensor testing system was then defined as the anatomic coordinate system of the glenohumeral joint.[7,8,14]

The initial joint orientation in the testing system was 60° of glenohumeral abduction, 0° of horizontal abduction, and 0° of external rotation. The horizontal abduction angle was held constant during the experimental protocol. Force control was then used to apply

a 22 N compressive load (medially directed) to the humerus while the forces in the two orthogonal directions were minimized (~0 N). This centered the humeral head within the glenoid cavity and determined the joint position at 60° of glenohumeral abduction and 0° of external rotation.[7,8,14]

A moment of 3 Nm was then applied to the humerus about its longitudinal axis while maintaining the 22 N joint compressive force to obtain the joint position corresponding to maximum external rotation. The identified joint position was 60° of glenohumeral abduction and 52° of external rotation (maximum achieved with 3 Nm rotation moment applied). At this joint orientation, a 25 N anterior load was applied to the humerus at the origin of its coordinate system, while maintaining the 22 N compressive force, and the resulting kinematics were recorded via the testing system. This protocol simulated the clinical exam to assess anterior stability of the glenohumeral joint.

A mechanical digitizing device (Microscribe 3DX, Immersion Corporation, San Jose, CA) was used to digitize three orthogonal surfaces of the registration blocks while the testing system rigidly held the joint at 60° of glenohumeral abduction, 52° of external rotation and the joint translations corresponding to a 25 N anterior load. The transformation matrix describing the relative location and orientation of the Plexiglas blocks attached to the humerus and scapula was then determined.[18] These data were used to prescribe the motion of the humerus with respect to the scapula for the finite element models. The motion tracking system was also utilized to record the location of the 77 strain markers affixed to the inferior glenohumeral ligament in the strained configuration.

With the location of the 77 markers known, it was then possible to calculate the maximum principal strain at the centroid of elements created by four neighboring strain markers or nodes was calculated. ABAQUS® (Student Version 6.4, Simulia, Providence, RI) was used to perform the calculations. First, the location of the markers in the reference strain configuration and the strained configuration were input as nodal locations for membrane elements.[29,30] A minimal thickness (0.02 mm) was assigned and an arbitrary constitutive model was selected since strain calculations are independent of constitutive model. The maximum principal strain (Green–Lagrange) of each element (created by four neighboring strain markers) was then determined at the centroid of each element while the direction of this maximum principal strain was determined at each node.

The geometry of the scapula, humerus and glenohumeral capsule was collected in the reference strain configuration using a computed tomography (CT) scanner (GE Lightspeed, Milwaukee, WI). Rubber tubes (diameter of 2 mm) were affixed to the margins of the anterior and posterior band of the inferior glenohumeral ligament using cyanoacrylate such that the ends of the tubes terminated at the insertion sites on the glenoid and humerus. This allowed regions of the capsule and their insertion sites to be visualized in the CT dataset. The joint was again fixed in the 6-degree of freedom plastic jig at the joint orientation corresponding to the reference strain configuration (60° of glenohumeral abduction, neutral horizontal abduction and 10° of external rotation). The plastic jig was placed within the CT scanner, the capsule was inflated to its reference configuration (5.2 kPa), and a CT dataset was collected (field of view = 180 mm, 100 kV, 120 mA, slice thickness = 1 mm, 512 × 512 pixels). The rubber tubes, Plexiglas blocks, strain markers, humerus, articular cartilage of the humerus, scapula, and capsular regions were all visible.

A combined experimental–computational approach was utilized to determine the material coefficients for the glenohumeral capsule based on an isotropic constitutive model.[12,16,32,37] Tissue samples were excised from each capsular region shown in Fig. 1. For the axillary pouch and posterior regions, two non-destructive tensile elongation and shear deformation loadings were applied to tissue samples (25 × 25 mm) in the directions parallel and perpendicular to the longitudinal axis of the capsular region. The longitudinal axis refers to the long axis of the tissue region which runs in the medial-to-lateral direction. Due to size limitations of the anterior and posterior bands of the inferior glenohumeral ligament and the anterosuperior region, it was only possible to excise tissue samples that were 5 × 15 mm. For these three regions, one non-destructive tensile elongation was applied to the tissue samples with respect to the axis that was parallel to the longitudinal axis of the capsular region. For all loading conditions, the clamp reaction force and clamp displacement were recorded.

Since the experimental material tests produced inhomogeneous deformations in the samples, the finite element method was used to simulate each experimental condition. The length, width, and thickness of the tissue sample were prescribed and the experimentally recorded elongation was used to drive the simulations. An inverse finite element optimization routine determined the material coefficients for an isotropic hypoelastic constitutive model that has been used previously to model the glenohumeral capsule.[16,37,39,45] Since two sets of coefficients were determined for the axillary pouch and posterior regions, the average of the material coefficients served as input to the finite element models (Table 1). Specific details regarding this optimization technique for the glenohumeral capsule can be found in Rainis *et al.*[37]

TABLE 1. Material coefficients for the isotropic hypoelastic constitutive model as determined from the mechanical testing protocol for all capsular regions.

Capsular region	E (MPa)	ν
AB-IGHL	2.05	0.4995
PB-IGHL	3.73	0.4995
Anterosuperior	2.12	0.4995
Axillary pouch	4.92	0.4995
Posterior	2.05	0.4995

Computational Methods

The geometry of the humerus, scapula, registration blocks, anterior and posterior bands of the inferior glenohumeral ligament, axillary pouch, anterior-superior, and posterior capsular regions were manually segmented in each slice of the CT dataset. (SURFdriver version 3.5.6, Hawaii) The surface definitions for the humerus, scapula, anterior and posterior bands of the inferior glenohumeral ligament, axillary pouch, anterior-superior, and posterior capsular regions, and the registration blocks were then imported into a finite element pre-processor. (TrueGrid, XYZ Scientific, Livermore, CA) Triangular surfaces representing the scapula, humerus and the articular cartilage of the humerus were converted directly to rigid body shell meshes.[16,27] The bursal side of the anterior and posterior band of the inferior glenohumeral ligament, axillary pouch, anterosuperior, and posterior capsular regions were meshed individually with quadrilateral shell elements.[22,23] The nodes along the edges of two adjacent meshes were then merged together. All capsular regions were included in the continuous model, while only the anterior and posterior bands of the inferior glenohumeral ligament and the axillary pouch were included in the discrete model. A 2 mm uniform thickness was prescribed for each capsular region.[4]

To determine the appropriate mesh to predict converged values of strain in the inferior glenohumeral ligament, the strain distribution within the glenohumeral capsule for three mesh densities was compared. Based on a previous study, a mesh of the capsule with 7530 elements was created.[16] Additionally, meshes with 1.5 times and two times the number of elements as the initial mesh were created. The model with 1.5 times the number of elements as the initial mesh produced average strains that were 1% less than the initial mesh. In contrast, the model with twice as many elements produced average strains that were only 0.1% less than the model with 1.5 times the number of elements. Therefore, the model with 1.5 times the elements as the initial mesh provided a balance between accuracy and computational expense, and this mesh was used for all analyses.

The Plexiglas blocks were used to co-register the experimentally collected kinematics and the position of the bones in the CT dataset.[18] Local coordinate systems were established on each block to define the position of the scapula and humerus with an accuracy of 0.1 mm. Motion was described using incremental translations and rotations[38] based on the experimental measurements. The nodes at the proximal and distal ends of the mesh of each capsular region were then rigidly fixed to that of the humerus and scapula.

Contact between the capsular regions and the humerus was prescribed via a frictionless sliding surface and contact was enforced using the penalty method.[16,28] No contact was observed between the capsular regions and the scapula; therefore, no contact was prescribed.

The non-linear finite element solver NIKE3D was used for all analyses.[1,13,16,19,20,44,46,47] Non-linear iterations were based on a quasi-Newton method[31] and convergence was based on the $L2$ displacement and energy norms.[27] The motions of the humerus with respect to the scapula were incrementally applied over quasi-time with the time step size being adjusted via an automatic procedure. LSPOST (Livermore Software Technology Corporation, Livermore, CA, USA) was used to visualize and output strains.

Data Analysis

To evaluate the predictions from the discrete and continuous finite element models, the predicted strain distributions and deformed shapes were compared to the experimental measurements. To allow a direct comparison, the strain markers attached to the glenohumeral capsule were segmented from the CT dataset and their locations were noted with respect to the mesh of each capsular region. Due to the size of the strain markers (1.6 mm) and the slice thickness (1.0 mm), it was difficult to identify all of the strain markers. Additionally, even though strain markers were visible in the CT dataset, it was not possible to determine its experimental counterpart since other strain markers may not have been visible. Thus only a subset of strain markers was accurately identified. Since the first column of strain markers was specifically placed anterior to a rubber tube, strain markers in this region were identifiable. With these complications, 11 sampling regions from the experimental strain dataset were available for comparisons (Fig. 3).

The elements of the computational mesh that were visually within an experimental strain sampling region were selected, and the predicted maximum principal Green–Lagrange strains were averaged over all elements. This average predicted value was compared to the strain in the corresponding experimental strain

sampling area. In order for the predicted strains to be considered valid, the average difference between the experimental and predicted strain values had to be within two times the repeatability of the experimental methodology used to determine the strain distribution in the glenohumeral capsule, or 7.0% strain. The experimental repeatability of determining the strain in the glenohumeral capsule was ±3.5% strain.

The predicted maximum principal strain for the glenoid and humeral portions of the inferior glenohumeral ligament were also evaluated for the continuous and discrete models. For each region of the inferior glenohumeral ligament, the elements traversing from the glenoid to the humeral insertion points were divided such that half the elements were assigned to the glenoid side and the opposing half were assigned to the humeral side. The average and standard deviation in maximum principal strain were then calculated for the glenoid and humeral sides in each region.

Additional qualitative analyses were performed to validate the predicted deformed shape of the capsular regions for the discrete and continuous models using photographs taken from an anteroinferior view. Experimentally, the shape of the capsular regions was obtained via images taken from the motion tracking system. In the computational environment, the discrete and continuous finite element models were oriented such that the perspective simulated that of the motion tracking system during experimental data collection. The manner in which the capsular regions wrapped around the humeral head was used to evaluate the ability of the discrete and continuous finite elements models to predict the deformed shape.

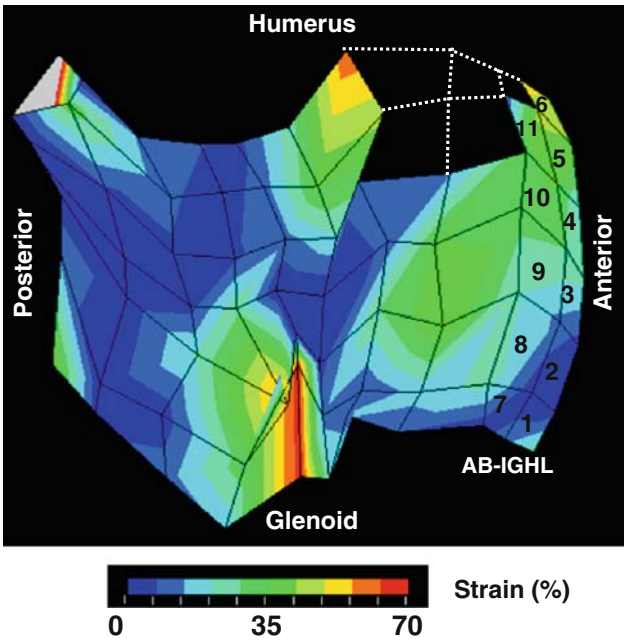

FIGURE 3. Inferior view of the left shoulder showing fringe plot of the maximum principal strain that was determined experimentally at maximum external rotation with 25 N anterior force applied to humerus. The 11 sampling regions of the anterior band of the inferior glenohumeral ligament (AB-IGHL) that were identified from experimental data are numbered. Dashed lines indicate missing markers.

RESULTS

Experimental Data

During the experimental protocol, three strain markers became completely detached from the capsule. These strain markers were located near the glenoid and on the anterior half of the axillary pouch. In addition, two strain markers were no longer rigidly affixed to the capsule, i.e. they were still on the capsule but could easily move around when gently palpated. Thus, the maximum principal strain could only be evaluated for 55 sampling regions (or elements created by a set of four neighboring strain markers) (Figs. 2 and 3). The average maximum principal strain from the 55 sampling regions of the inferior glenohumeral ligament was 14.3 ± 15.5% and the peak strain was 54.9%. However, difficulty was experienced when attempting to view these strain markers in the CT images which was necessary to determine the computational elements associated with each experimental element. Figure 3 shows the 11 experimental elements that could also be identified in the CT scan.

Computational Data

Comparisons of the predicted maximum principal strains between the continuous and discrete models showed several differences (Figs. 4 and 5). For the glenoid side of each capsular region, the predicted strains were larger for the continuous model when compared to the discrete model for the AB-IGHL and axillary pouch. In fact, an average difference of 40% was found in the predicted strain for the AB-IGHL. The range of the strain predicted for the discrete and

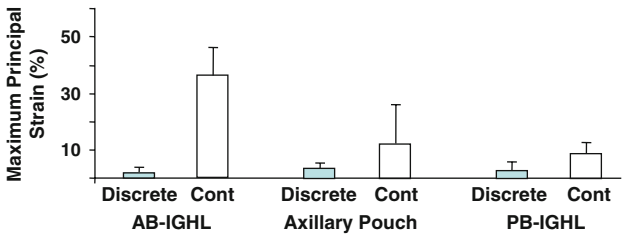

FIGURE 4. Maximum principal strain predicted by the continuous and discrete models for the glenoid side of each capsular region within the inferior glenohumeral ligament (mean ± SD).

continuous finite element models in these regions was 0–7% and 9–55%, respectively. When evaluating the glenoid side of the axillary pouch, the average predicted strains were similar between the two models. However, the range for the discrete model was 0–12% while it was 0–85% for the continuous model. For the PB-IGHL, the predicted strains on the glenoid side were similar between the two models, with average strains that were less than 10%. The range in predicted strain was also similar at 0–14% for the discrete model and 1–17% for the continuous model.

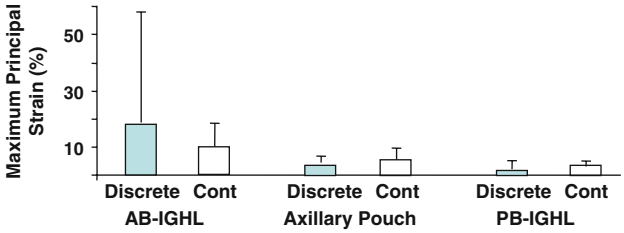

FIGURE 5. Maximum principal strain predicted by the continuous and discrete models for the humeral side of each capsular region within the inferior glenohumeral ligament (mean ± SD).

With the exception of the AB-IGHL in the discrete model, all average strain values were less than 10% on the humeral side. The average strain for the AB-IGHL in the discrete model approached 20% due to the existence of the unrealistic strain (437%) near its humeral insertion (range 0–437%). For the continuous model, a range of only 0–37% existed for this region. No strains exceeded 18% for the discrete and continuous models in the axillary pouch and posterior band of the inferior glenohumeral ligament regions.

The predicted deformed shapes for the discrete and continuous models were clearly different (Fig. 6). In the continuous model, the anterosuperior region and the AB-IGHL both wrapped around the humeral head with larger strains near the glenoid side of the tissue. Portions of the superior region on the glenoid side were in an "elevated" position from the humeral head—approximating the shape in its reference strain configuration. Thus, there was no contact with the humeral head for this portion of the capsule. For the discrete model, the AB-IGHL buckled away from the humeral head and made no contact with its articular surface. Therefore, small strains (~5%) were predicted across the entire inferior glenohumeral ligament with the exception of the large strain at the insertion point of 437%.

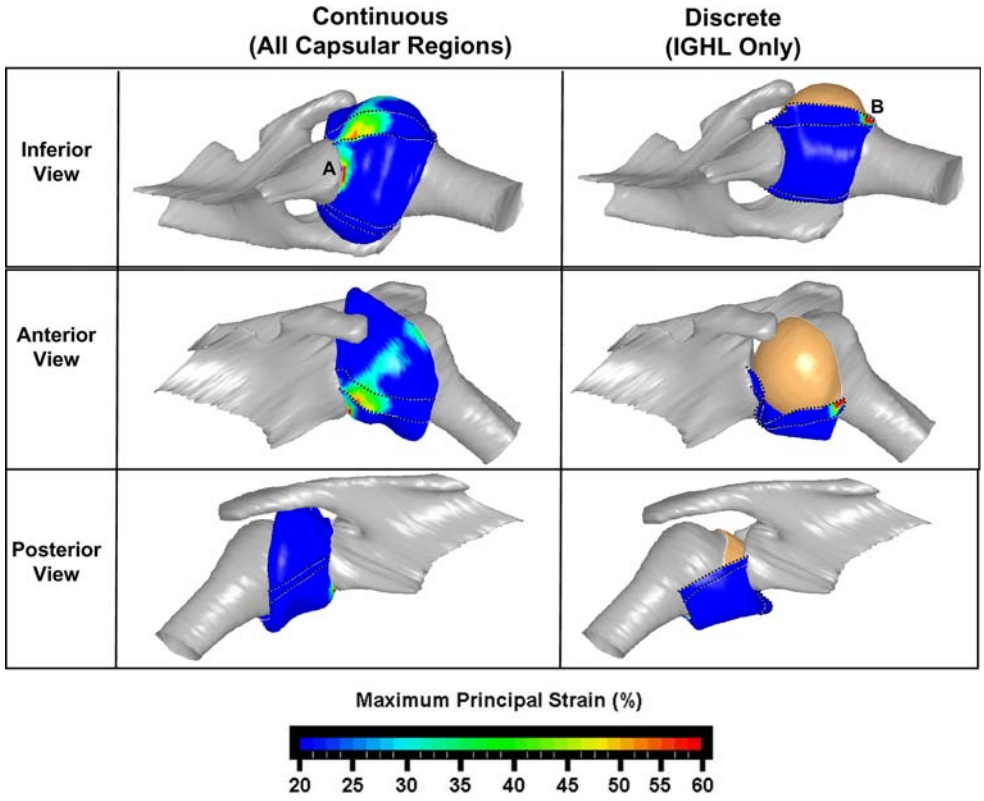

FIGURE 6. Inferior, anterior, and posterior views of maximum principal strains and deformed shapes for the left shoulder predicted by continuous and discrete finite element models where points A and B indicate strains of 85 and 437%, respectively, which are outside the bounds of the scale.

Validation

The comparisons for the experimental measurements and the predicted results for the discrete model showed large differences between the strain distribution and deformed shape. Only five of the experimental sampling regions consisted of tissue that was located exclusively in the inferior glenohumeral ligament due to the position of the first row of strain markers. Therefore, sampling regions 7–11 were utilized for comparison purposes with the discreet model. The discrete model did not accurately predict the strains for these elements with an average difference between the experimental and predicted values of 17% strain (Fig. 7). The deformed shape observed experimentally showed that the anterosuperior region, AB-IGHL, and anterior portion of the axillary pouch all wrap around the humeral head (Fig. 8).

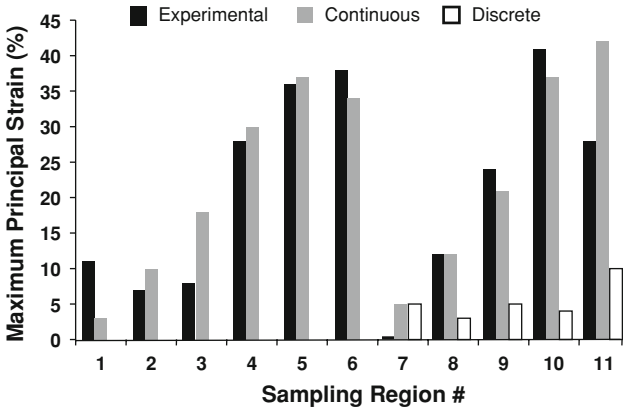

FIGURE 7. Maximum principal strain from the experimental measurements as well as predicted by the continuous and discrete models for each sampling region. Note that values for the discrete model are only provided for sampling regions 7 to 11.

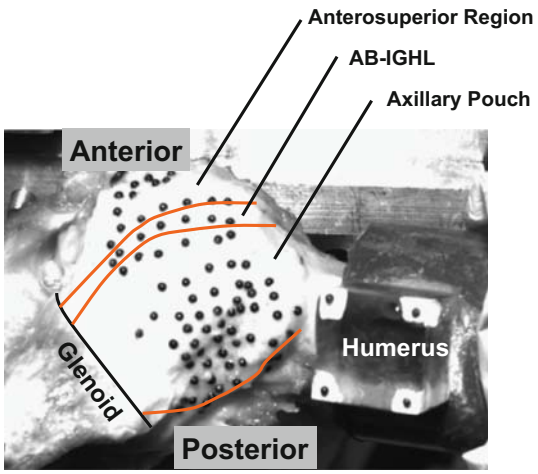

FIGURE 8. Inferior view of the left shoulder during experimental data collection in the strained configuration (60° abduction, maximum external rotation, and 25 N anterior force applied to humerus.

In contrast, the average difference between the predicted strain values from the continuous model and the experimental data was less than 5%. Therefore, the predicted strain distribution was within the validation criteria of 7.0%. The validation criteria were satisfied even though the differences between the predicted and experimental strain data for 3 of the 11 sampling regions were greater than 8%. Furthermore, the deformed shape was correctly predicted by the continuous model with the capsular regions correctly wrapping around the humeral head (Figs. 6 and 8).

DISCUSSION

This study compared the predicted strain distribution and deformed shape of the inferior glenohumeral ligament for two finite element models (continuous model and discrete model) with values based on experimental measurements. The experimental strain distribution was similar to previously reported measurements for the same loading conditions with larger strains near the glenoid side of the AB-IGHL, axillary pouch, and inferior portion of the anterosuperior region.[34]

For the inferior glenohumeral ligament, the predicted strains and deformed shape of the continuous model were validated. The average difference from the experimentally measured strains was less than 5% and no differences were observed in deformed shape for the 11 experimental sampling regions. However, the data presented in this study clearly indicate that a discrete model of the IGHL was not appropriate for this joint position and loading condition as it failed to predict accurate strains and the deformed shape. Thus, excluding neighboring capsular regions greatly affected the predicted results.

Due to the significant challenges in regards to the numerical simulation, previous studies typically evaluated the function of the glenohumeral capsule as discrete structures. The results suggest that the regions of the capsule frequently described in the literature as glenohumeral ligaments have significant interactions when transferring forces between the scapula and humerus unlike traditional ligaments. When assessing the function of the glenohumeral capsule, isolated, discrete capsular regions should not be used in experimental or computational analyses. Instead, the glenohumeral capsule should be evaluated as a continuous sheet of fibrous tissue. Isolating the glenohumeral capsule into discrete capsular regions drastically alters the interactions between each region of the capsule. Thus, the loads transmitted by each isolated capsular region would not be representative of that observed when all capsular regions are included. Altering the load

transmission characteristics of a capsular region would also result in inaccurate stress and strain distributions. The function of a capsular region in providing joint stability could then be determined incorrectly.

The current work clearly indicates that the glenohumeral capsule should be evaluated as a continuous sheet of fibrous tissue. However, experimentally evaluating the forces transmitted to the humeral head via the glenohumeral capsule and evaluating the mechanical properties pose many experimental difficulties. Despite these difficulties, a thorough understanding of the function of the glenohumeral capsule and its capsular regions is necessary to improve patient outcomes. Improving the understanding of capsular function will also allow surgeons to assess the function of the repaired capsule post-operatively. Thus, there exists a need to continue to develop and validate subject-specific continuous finite element models. Multiple models should be developed that are representative across the population. These validated subject-specific, continuous finite element models could then be utilized to evaluate the mechanisms that the capsular regions utilize to transfer load from the humerus to the scapula at various joint positions and to provide joint stability.

The results from this study also suggest that surgeons may need to consider the complex interactions between each capsular region that exist in the uninjured state while attempting to restore normal function. These interactions between regions of the glenohumeral capsule can be evaluated in more detail via multiple validated subject-specific continuous finite element models. Additionally, the stress and strain distributions would provide a means for identifying locations within the glenohumeral capsule that are at risk for injury and could be assessed for various joint positions. Moreover, these models could be utilized to simulate the effect of diminished mechanical properties of the capsular regions on the resulting stress, strain, and force transmission capabilities based on cadaveric investigations. Mechanical properties may be diminished due to several factors such as aging,[25] disease, or surgical repair procedures that alter the mechanical properties of the capsular regions such as thermocapsular shrinkage.[11,26] Finally, these models could be utilized to investigate the effects of performing surgical repairs at various joint orientations immediately following surgery or while applying a variety of loading conditions to the joint. Thus, utilizing these models to simulate the normal, injured, and repaired state, would provide scientific rationale to improve clinical exams for diagnosis and surgical planning, surgical repair techniques, and would enhance our understanding of normal function.

An isotropic hypoelastic constitutive model was used to represent the glenohumeral capsule; and the predicted strain and deformed shape were validated for the continuous model. However, incorporating a hyperelastic constitutive model could potentially improve the agreement between the experimental data and computational predictions as it would allow for non-linear behavior of the capsule. Furthermore, the behavior of the quadrilateral shell elements can support bending, which is not physiological for the capsular tissue. For validation purposes, the average error between the experimental and predicted strain values across the glenohumeral capsule was utilized. Thus, while the average error was less than two times the experimental error (7%), the error at each location evaluated on the glenohumeral capsule was not always less than 7%. Even though only one subject-specific finite element model of the glenohumeral capsule was constructed, significant differences existed between the continuous and discrete models that were sufficient to answer the research question. In addition, only the inferior glenohumeral ligament was used for comparison purposes. However, the predicted deformed shape at the superior margin of the anterosuperior region near the glenoid was unrealistic in the continuous model with this tissue being elevated away from the humeral head. Applying a gravitational force might result in a more realistic predicted deformed shape for the anteriosuperior region of the capsule as it was not loaded in any other way for the joint positions investigated in this study. An unreasonably high strain was identified where the anterior band inserts into the humeral head. These high strains were probably due to the lack of the remaining capsule to apply loads to the tissue and neglecting to properly model the complex insertion of the capsule into the humerus and glenoid. Therefore, modeling the insertion sites of the capsule properly will be examined in the future. In addition, the strain distribution near the attachment points should be interpreted carefully when using this model. Finally, the effects of intracapsular pressure were neglected in our experimental and computation models since the joint was vented. Thus, the magnitude of translation and shape of the capsule could have been altered compared to *in vivo* conditions.

This study clearly demonstrates the complexity of the glenohumeral capsule and the need for further research. In the future, inclusion of the labrum should also be considered since it may result in decreased strains at the insertion sites. Future investigations will include the development of multiple subject-specific finite element models that represent a population of individuals. The effect of using only a discrete model of the glenohumeral capsule to predict the resulting joint kinematics when external forces and moments are applied to the joint could also be examined.

ACKNOWLEDGMENT

The support of NIH grants AR-050218 and AR-047369 is gratefully acknowledged.

REFERENCES

[1]Anderson, A. E., C. L. Peters, B. D. Tuttle, and J. A. Weiss. Subject-specific finite element model of the pelvis: development, validation and sensitivity studies. *J. Biomech. Eng*. 127:364–373, 2005.

[2]Arciero, R. A., J. H. Wheeler, J. B. Ryan, and J. T. McBride. Arthroscopic Bankart repair versus nonoperative treatment for acute, initial anterior shoulder dislocations. *Am. J. Sports Med*. 22:589–594, 1994.

[3]Baker, C. L., J. W. Uribe, and C. Whitman. Arthroscopic evaluation of acute initial anterior shoulder dislocations. *Am. J. Sports Med*. 18:25–28, 1990.

[4]Bigliani, L. U., R. G. Pollock, L. J. Soslowsky, E. L. Flatow, R. J. Pawluk, and V. C. Mow. Tensile properties of the inferior glenohumeral ligament. *J. Orthop. Res*. 10:187–197, 1992.

[5]Boardman, N. D., R. E. Debski, J. J. Warner, E. Taskiran, L. Maddox, A. B. Imhoff, F. H. Fu, and S. L.-Y. Woo. Tensile properties of the superior glenohumeral and coracohumeral ligaments. *J. Shoulder Elbow Surg*. 5:249–254, 1996.

[6]Brenneke, S. L., J. Reid, R. P. Ching, and D. L. Wheeler. Glenohumeral kinematics and capsulo-ligamentous strain resulting from laxity exams. *Clin. Biomech*. 15:735–742, 2000.

[7]Burkart, A. C., and R. E. Debski. Anatomy and function of the glenohumeral ligaments in anterior shoulder instability. *Clin. Orthop. Relat. Res*. 400:32–39, 2002.

[8]Burkart, A., R. E. Debski, V. Musahl, and P. J. McMahon. Glenohumeral translations are only partially restored after repair of the type II SLAP lesion. *Am. J. Sports Med*. 31:56–63, 2003.

[9]Caspari, R. B. Arthroscopic reconstruction for anterior shoulder instability. *Tech. Orthopaed*. 3:59–66, 1988.

[10]Cave, E., J. Burke, and R. Boyd. Trauma Management. Chicago, IL: Year Book Medical Publishers, p. 437, 1974.

[11]Chen, S., P. S. Haen, J. Walton, and G. A. Murrell. The effects of thermal capsular shrinkage on the outcomes of arthroscopic stabilization for primary anterior shoulder instability. *Am. J. Sports Med*. 33:705–711, 2005.

[12]Debski, R. E., S. M. Moore, J. L. Mercer, M. S. Sacks, and P. J. McMahon. The collagen fibers of the anteroinferior capsulolabrum have multiaxial orientation to resist shoulder dislocation. *J. Shoulder Elbow Surg*. 12:247–252, 2003.

[13]Debski, R. E., J. A. Weiss, W. J. Newman, S. M. Moore, and P. J. McMahon. Stress and strain in the anterior band of the inferior glenohumeral ligament during a simulated clinical examination. *J. Shoulder Elbow Surg*. 14:24S–31S, 2005.

[14]Debski, R. E., E. K. Wong, S. L.-Y. Woo, M. Sakane, F. H. Fu, and J. J. Warner. In situ force distribution in the glenohumeral joint capsule during anterior-posterior loading. *J. Orthop. Res*. 17:769–776, 1999.

[15]Deutsch, A., J. E. Barber, D. T. Davy, and B. N. Victoroff. Anterior-inferior capsular shift of the shoulder: a biomechanical comparison of glenoid-based versus humeral-based shift strategies. *J. Shoulder Elbow Surg*. 10:340–352, 2001.

[16]Ellis, B. J., R. E. Debski, S. M. Moore, P. J. McMahon, and J. A. Weiss. Methodology and sensitivity studies for finite element modeling of the inferior glenohumeral ligament complex. *J. Biomech*. 40:603–612, 2007.

[17]Field, L. D., D. J. Bokor, and F. H. Savoie, 3rd. Humeral and glenoid detachment of the anterior inferior glenohumeral ligament: a cause of anterior shoulder instability. *J. Shoulder Elbow Surg*. 6:6–10, 1997.

[18]Fischer, K. J., T. T. Manson, H. J. Pfaeffle, M. M. Tomaino, and S. L. Woo. A method for measuring joint kinematics designed for accurate registration of kinematic data to models constructed from CT data. *J. Biomech*. 34:377–383, 2001.

[19]Gardiner, J. C., and J. A. Weiss. Simple shear testing of parallel-fibered planar soft tissues. *J. Biomech*. 123:1–5, 2001.

[20]Gardiner, J. C., and J. A. Weiss. Subject-specific finite element models can predict strain in the human medial collateral ligament during valgus knee loading. *J. Orthop. Res*. 21:1098–1106, 2003.

[21]Hawkins, R. J., and N. G. Mohtadi. Controversy in anterior shoulder instability. *Clin. Orthop. Relat. Res*. 272:152–161, 1991.

[22]Hughes, T. J. R., and W. K. Liu. Nonlinear finite element analysis of shells: part I. Two-dimensional shells. *Comput. Methods Appl. Mech. Eng*. 27:167–181, 1981.

[23]Hughes, T. J. R., and W. K. Liu. Nonlinear finite element analysis of shells: part II. Three-dimensional shells. *Comput. Methods Appl. Mech. Eng*. 27:331–362, 1981.

[24]Itoi, E., J. J. Grabowski, B. F. Morrey, and K. N. An. Capsular properties of the shoulder. *Tohoku J. Exp. Med*. 171:203–210, 1993.

[25]Lee, T. Q., J. Dettling, M. D. Sandusky, and P. J. McMahon. Age related biomechanical properties of the glenoid-anterior band of the inferior glenohumeral ligament-humerus complex. *Clin. Biomech*. 14:471–476, 1999.

[26]Levine, W. N., L. U. Bigliani, and C. S. Ahmad. Thermal capsulorrhaphy. *Orthopedics* 27:823–826, 2004.

[27]Maker, B. N. Rigid Bodies for Metal Forming Analysis with NIKE3D. University of California, Lawrence Livermore Laboratory, 1995, pp. 1–8.

[28]Maker, B. N., R. M. Ferencz, and J. O. Hallquist, NIKE3D: A Nonlinear, Implicit, Three-Dimensional Finite Element Code for Solid and Structural Mechanics. Lawrence Livermore National Laboratory, 1990.

[29]Malicky, D. M., J. E. Kuhn, J. C. Frisancho, S. R. Lindholm, J. A. Raz, and L. J. Soslowsky. Neer Award 2001: nonrecoverable strain fields of the anteroinferior glenohumeral capsule under subluxation. *J. Shoulder Elbow Surg*. 11:529–540, 2002.

[30]Malicky, D. M., L. J. Soslowsky, J. E. Kuhn, M. J. Bey, C. M. Mouro, J. A. Raz, and C. A. Liu. Total strain fields of the antero-inferior shoulder capsule under subluxation: a stereoradiogrammetric study. *J. Biomech. Eng*. 123:425–431, 2001.

[31]Matthies, H., and G. Strang. The solution of nonlinear finite element equations. *Int. J. Numer. Methods Eng*. 14:1613–1626, 1979.

[32]Moore, S. M., P. J. McMahon, E. Azemi, and R. E. Debski. Bi-directional mechanical properties of the posterior region of the glenohumeral capsule. *J. Biomech*. 38:1365–1369, 2005.

[33]Moore, S. M., P. J. McMahon, and R. E. Debski. Bi-directional mechanical properties of the axillary pouch

of the glenohumeral capsule: implications for surgical repair. *J. Biomech. Eng*. 126:284–288, 2004.
[34]Moore, S. M., J. H. Stehle, E. J. Rainis, P. J. McMahon, and R. E. Debski. The current anatomical description of the inferior glenohumeral ligament does not correlate with its functional role in positions of external rotation. *J. Orthop. Res*. 26:1598–1604, 2008.
[35]Morgan, C. D., and A. B. Bodenstab. Arthroscopic Bankart suture repair: technique and early results. *Arthroscopy* 3:111–122, 1987.
[36]Novotny, J. E., B. D. Beynnon, and C. E. Nichols. Modeling the stability of the human glenohumeral joint during external rotation. *J. Biomech*. 33:345–354, 2000.
[37]Rainis, E. J., S. A. Maas, H. B. Henninger, P. J. McMahon, J. A. Weiss, and R. E. Debski. Material properties of the axillary pouch of the glenohumeral capsule: Is isotropic material symmetry appropriate? *J. Biomech. Eng*. 131: 031007, 2009.
[38]Simo, J. C. On the dynamics in space of rods undergoing large motions: a geometrically exact approach. *Comput. Methods Appl. Mech. Eng*. 66:125–161, 1988.
[39]Simo, J. C., and T. J. R. Hughes. Computational Inelasticity. New York: Springer, 1998.
[40]Speer, K. P., X. Deng, P. A. Torzilli, D. A. Altchek, and R. F. Warren. Strategies for an anterior capsular shift of the shoulder. A biomechanical comparison. *Am. J. Sports Med*. 23:264–269, 1995.
[41]Sperber, A., P. Hamberg, J. Karlsson, L. Sward, and T. Wredmark. Comparison of an arthroscopic and an open procedure for posttraumatic instability of the shoulder: a prospective, randomized multicenter study. *J. Shoulder Elbow Surg*. 10:105–108, 2001.
[42]Ticker, J. B., L. U. Bigliani, L. J. Soslowsky, R. J. Pawluk, E. L. Flatow, and V. C. Mow. Inferior glenohumeral ligament: geometric and strain-rate dependent properties. *J. Shoulder Elbow Surg*. 5:269–279, 1996.
[43]Warren, R. F. Subluxation of the shoulder in athletes. *Clin. Sports Med*. 2:339–354, 1983.
[44]Weiss, J. A., and J. C. Gardiner. Computational modeling of ligament mechanics. *Crit. Rev. Biomed. Eng*. 29:303–371, 2001.
[45]Weiss, J. A., J. C. Gardiner, and C. Bonifasi-Lista. Ligament material behavior is nonlinear, viscoelastic and rate-independent under shear loading. *J. Biomech*. 35:943–950, 2002.
[46]Weiss, J. A., B. N. Maker, and S. Govindjee. Finite element implementation of incompressible, transversely isotropic hyperelasticity. *Comput. Methods Appl. Mech. Eng*. 135: 107–128, 1996.
[47]Weiss, K. S., and F. H. Savoie, 3rd. Recent advances in arthroscopic repair of traumatic anterior glenohumeral instability. *Clin. Orthop. Relat. Res*. 400:117–122, 2002.